Korean J. Chem. Eng., 39(10), 2725-2735 (2022)
DOI: 10.1007/s11814-022-1172-6

pISSN: 0256-1115
eISSN: 1975-7220

Comparative study of naproxen degradation via integrated UV/O$_3$/PMS process: Degradation products, reaction pathways, and toxicity assessment

Mojtaba Pourakbar*, Farshid Ghanbari, Amir Hossein Cheshme Khavar***, Maryam Khashij****,**
Mohammad Mehralian**, Ali Behnami*,*****, Mohammad Satari******,**
Mostafa Mahdaviapour, Ali Oghazyan*******, and Ehsan Aghayani**,†**

*Department of Environmental Health Engineering, Maragheh University of Medical Sciences, Maragheh, Iran
**Research Center for Environmental Contaminants (RCEC), Abadan University of Medical Sciences, Abadan, Iran
***Department of Chemistry, Farhangian University, Tehran, Iran
****Department of Environmental Health Engineering, Shahid Sadoughi University of Medical Sciences, Yazd, Iran
*****Department of Environmental Health Engineering, Iran University of Medical Sciences, Tehran, Iran
******Department of Biophysics, Faculty of Biological Sciences, Malayer University, Malayer, Iran
*******Department of Environmental Health Engineering, School of Health,
Sabzevar University of Medical Sciences, Sabzevar, Iran

(*Received 2 February 2022 • Revised 11 May 2022 • Accepted 11 May 2022*)

Abstract−The present study comprehensively investigated the degradation of naproxen (NPX) using UV/O$_3$/peroxymonosulfate (PMS), UV/O$_3$, UV/PMS, and O$_3$/PMS processes. The effects of various parameters such as PMS and ozone dosage, pH, and NPX concentration were investigated on process performance. Scavenging tests were conducted to identify the dominant radical species. The results under the optimal conditions show that the UV/O$_3$/PMS process is highly efficient for NPX degradation within 30 min of reaction time. Synergy index was also calculated and it was found that ozonation of the UV/PMS process leads to higher removal efficiency and a synergy effect of about 25% was calculated. It was also found that after complete destruction of NPX molecules, 76.9% of TOC was also removed. The final degradation by-products was tracked and it was proved that hydroxylation and decarboxylation were the main pathways in NPX degradation in the UV/O$_3$/PMS reactor. It was also proved that $^{\bullet}$OH was the main oxidizing agent in the UV/O$_3$/PMS and accordingly the degradation mechanism of NPX was suggested. Cytotoxicity assessment of the process effluent indicated a noticeable reduction in the toxicity of the NPX-laden solution after treatment using UV/O$_3$/PMS process. Furthermore, cost analysis of the different oxidation processes for real wastewater indicated that UV/O$_3$/PMS is the most cost-effective process compared to that of other processes (112 US\$/m^3). Accordingly, it can be put forth that the UV/O$_3$/PMS process is a promising and reliable process for the degradation of naproxen.

Keywords: Advanced Oxidation, Cytotoxicity, Ozone, Pharmaceutical, Radical Species

INTRODUCTION

Naproxen (NPX), as a conventional anti-inflammatory of non-steroidal drug, is detected in effluents discharged from the wastewater treatment plant. NPX concentrations in these effluents have been reported from 25 ng L^{-1} to 33.9 μg L^{-1} [1,2]. Due to incomplete decomposition, NPX is constantly detected in groundwater, surface water and drinking water. The negative eco-toxicological effect of naproxen on human embryonic cells has been reported in a toxicological studies [1]. Unfortunately, the conventional treatment processes for efficient removal of NPX are far from satisfactory in a short treatment period and therefore it is essential to find other processes to remove this contaminant from aqueous environment [3]. Advanced oxidation processes (AOPs) are among promising technologies for the management of emerging pollutants by the generation of singlet oxygen ($^{\bullet}$O), Hydroxyl radical ($^{\bullet}$OH), and sulfate radical (SO$_4^{\bullet-}$), namely as reactive oxygen species (ROSs) [4]. $^{\bullet}$OH destroys a broad range ligand of the organic compounds quickly and pervasively [5]. Also, SO$_4^{\bullet-}$ produced by peroxymonosulfate (HSO$_5^-$, PMS) activation can intensify the decomposition ligand of the organic compounds [6]. To generate free radicals, ultraviolet (UV) radiation as one of the economical and common forms of energy has been proven effective for PMS and different oxidants activation [7].

Based on the previous reports, both $^{\bullet}$OH and SO$_4^{\bullet-}$ radicals contributed to the degradation of contaminants in the UV/O$_3$/PMS process [8]. The simultaneous application of $^{\bullet}$OH and SO$_4^{\bullet-}$ has been studied for degradation of acesulfame [9], iopamidol [10], acetaminophen [11], ibuprofen [12], and chloramphenicol [13]. Lin et al. [14] reported a removal efficiency of 95.2% and the degradation rate constant (k_{app}) of 0.145 min^{-1} for Bisphenol A (BPA) in ozone-based AOPs (VUV/UV/PMS) via contribution of ROSs. Furthermore, the relative contributions of ROS in the UV/O$_3$/PMS process were evaluated based on the steady-state consumption to calculate the trace organic contaminants degradation in water and wastewater [15]. Thus, combining UV, O$_3$, and PMS (UV/O$_3$/PMS)

---

†To whom correspondence should be addressed.
E-mail: e.aghayani@abadanums.ac.ir

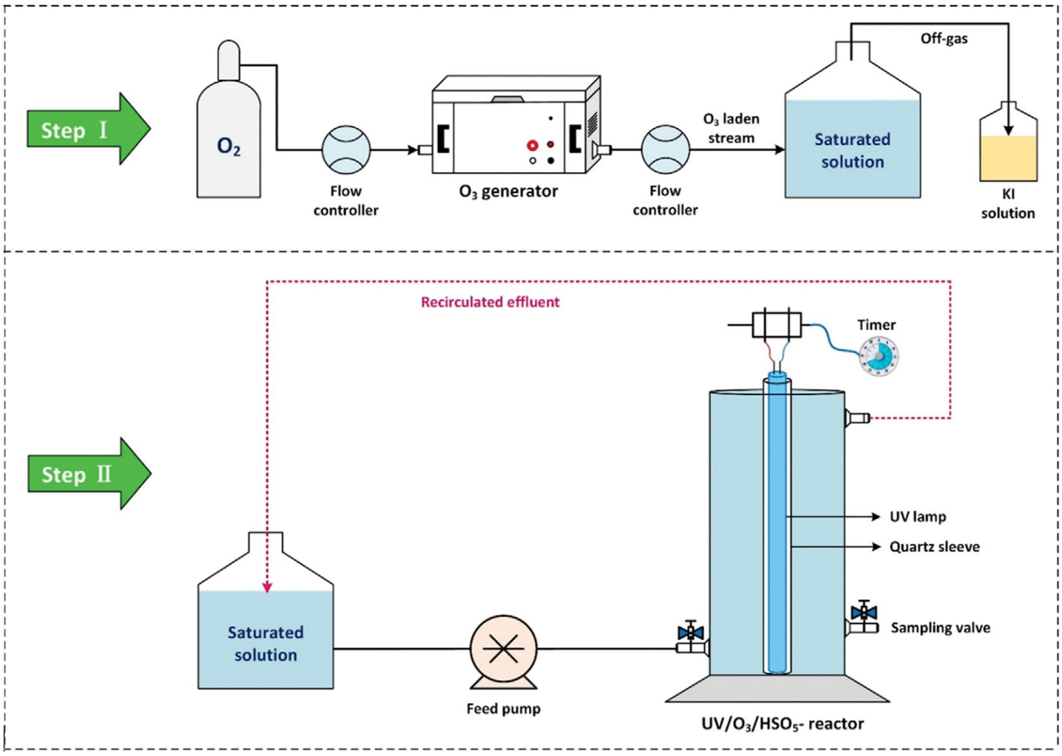

Fig. 1. The schematic of the UV/O_3/PMS reactor.

could–simultaneously activate O_3 molecule to generate ${}^{\bullet}OH$ and HSO_5^- to $SO_4^{\bullet-}$, to achieve stronger oxidants rather than initial molecules. Application of this method can lead to a unique synergistic effect for PMS activation.

Although the efficiency of $SO_4^{\bullet-}$ and ${}^{\bullet}OH$ in the degradation of NPX has been investigated under different conditions, it is first to comprehensively present the radical generations in the UV/O_3/PMS process for antibiotics degradation. For this purpose, the crucial operating parameters of PMS and ozone dosage, initial NPX concentration, and pH were investigated. In addition, the efficacy of different combinations of the determining agents (UV/O_3/PMS, UV/O_3, PMS/O_3, UV/PMS, Ozone, PMS, and UV alone) for NPX degradation were investigated. Furthermore, the oxidation mechanism of NPX was thoroughly studied based on the proposed degradation by-products. Then, kinetic modeling was conducted by approved transition metals (cobalt, and iron) on NPX removal. Finally, the degradation pathway for NPX in UV/O_3/PMS process was suggested.

MATERIALS AND METHODS

1. Reagents

All materials used in the present study were of analytical grade and used without any further purification. The stock solutions were daily prepared using deionized water from a Milli-Q Academic water purification system. NPX (purity>99.0%) was purchased from Iran Drug Co. Potassium peroxymonosulfate ($KHSO_5$), ferrous sulfate ($FeSO_4$), cobalt chloride ($CoCl_2$), and methanol (HPLC grade) were purchased from Sigma-Aldrich.

2. Experimental Procedure

To investigate the photocatalytic performance of the UV/O_3/PMS process for degradation of NPX, a 500 mL quartz reactor was fabricated. A schematic of the photoreactor is displayed in Fig. 1. The volume of synthetic solutions for each run was 300 mL. An ozone generator (Arda, Ozoneuf, Model COG 40A, France) generated the O_3 using pure oxygen as a feed with a nominal capacity of 1 g/h. For control and measurement of ozone gas, a mass flow meter was used. The off-gas ozone from the reactor was trapped in containers of potassium iodide (KI) solution. The UV light source (Philips Co.) was a 16 W low-pressure mercury lamp at wavelength of 254 nm, which was placed at the center of the reactor. In addition, $KHSO_5$, as a source for sulfate radical generation, in the range of 0.1 to 2.66 mM L^{-1}, was injected into the reactor. All the experiments were conducted in duplicate and the mean values along with standard deviations are reported.

3. Analytical Methods

The concentrations of COD and TOC were obtained based on the standard methods [16]. TOC was determined with a TOC analyzer (Liqui TOC II, Elementar, Germany). The removal efficiency was calculated using the following equation:

$$\%R = \frac{C_i - C_f}{C_i} \times 100 \tag{1}$$

where, C_i and C_f are initial and final concentrations of each parameter, respectively. The NPX concentration was determined with HPLC (Shimadzu HPLC LC-2010AHT, Japan). The intermediates of NPX degradation were also identified by LC-MS (positive ion mode ESI mass spectra).

4. Cytotoxicity Assessment

The MTT (dimethylthiazol-diphenyltetrazolium bromide) colorimetric assay was used for cytotoxicity assessment as previously explained [17]. Briefly, human embryonic kidney cells (HEK 293 cells) were obtained from National Cell Bank of Iran (NCBI) and maintained at 37 °C under 5% CO_2 and 100% humidity in DMEM and supplemented with 10% fetal calf serum. To be more accurate in the results, the medium was papered daily. The confluence cells was trypsinized and plated in 96-cluster well culture plates. The concentration of cells was 1×10^4 cells/well. Then, the plates were incubated for 24 h while each well contained 100 µl of cell suspension. The incubation was conducted under 5% CO_2 at 37 °C. After incubation, the old medium was discharged and replaced with 100-µl of new media containing different concentrations of NPX and NPX outflow. Cells treated with medium only were attended as the control group, and cells were incubated for 24 and 48 h. Separately, MTT stock was prepared by dissolving 5 mg MTT per ml of PBS and filtered through a 0.22 µm filter before diluting with DMEM at the concentration of 10% v/v. Following the incubation period under above-mentioned situation, 100 µl of MTT reagent (0.5 mg/ml) was added to each well of plates and they were incubated for another 4 h. Then, 100 µl of DMSO was added after the MTT solution had been discarded. To solubilize the formation of purple crystal formazan, the plates were placed on a shaker. Finally, cytotoxicity assessment of the cells was determined by the absorbance at a wavelength of 540 nm using a microplate reader. The results were interpreted with a graph that was obtained with cell viability against extract concentrations.

RESULTS AND DISCUSSION

1. NPX Degradation by Different Oxidation Processes

The degradation efficiency of NPX by different oxidation processes was compared with integrated UV/O$_3$/PMS process. As shown in Fig. 2, the NPX removal efficiency in the UV/O$_3$/PMS, UV/PMS, O$_3$/PMS, UV/O$_3$, and O$_3$ alone processes was achieved 100%, 65%, 84%, 85% and 22%, respectively. UV alone radiation and PMS alone exhibited negligible degradation of NPX, and it is confirmed that the integrated UV/O$_3$/PMS process for NPX degradation displayed a remarkable enhanced efficiency compared with other processes, which is due to the superlative synergistic effect [18]. To better illustrate the synergistic effect of ozonation of the UV/PMS process for NPX degradation, the following equation was used:

$$\text{Synergistic effect (\%)}=\text{NPX \% removal in UV/O}_3\text{/PMS} - (\text{NPX \% removal in UV/PMS}+\text{NPX \% removal in O}_3\text{ alone}) \quad (2)$$

Based on the results and various combinations of the processes, it is found that ozonation of the UV/PMS process for 30 min leads to 25% of synergistic effect in NPX removal. Cuerda-Correa et al. [19] reviewed the advanced oxidation processes for the removal of antibiotics in various oxidation processes. A considerable synergistic effect was observed when the reactions were performed by an integrated system. Qin et al. [20] revealed that the UV/O$_3$/Peroxydisulfate (PDS) process displayed superiority for the degradation of clofibric acid (CA) in comparison with other processes. They reported that integrated UV/O$_3$/PDS process increased the CA destruction ratio from 1.7 to 1.9. Also, the combination UV, H_2O_2, and O_3 showed outstanding operations for the elimination precursors of haloacetonitrile (HAN), which were the most effective rather than other combined processes such as O_3/H_2O_2 and UV/O$_3$ processes [21]. Results of present study are clarifying that enhanced destruction of pollutants could be reached by simultaneous generation of $^{\bullet}OH$ and $SO_4^{\bullet-}$ radicals in the UV/O$_3$/PMS process, as a significant potential alternative process for the efficient removal of organic emerging pollutants.

2. Effects of Parameters in UV/O$_3$/PMS Process

2-1. Effect of Solution pH

One of the most important parameters in PMS-based AOPs is the pH of solution. There are remarkably crucial influences on the formation of ROSs type, the molar absorption of HSO_5, and the

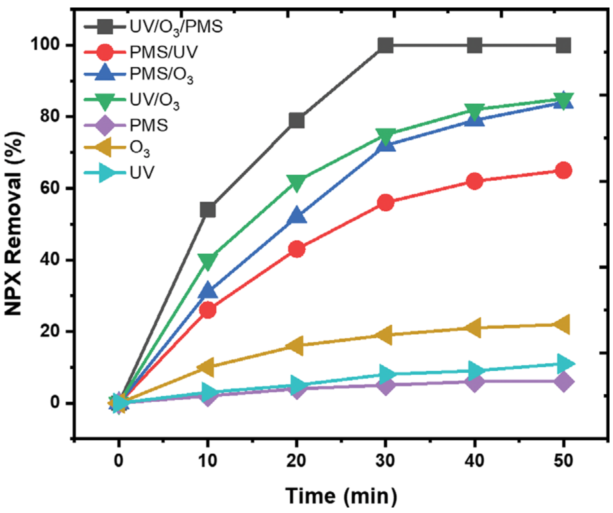

Fig. 2. The removal efficiencies of NPX in different processes (O$_3$ dosage=8.2 mg/L, PMS dosage=1.68 mM/L, NPX concentration=5 mg/L, pH=5).

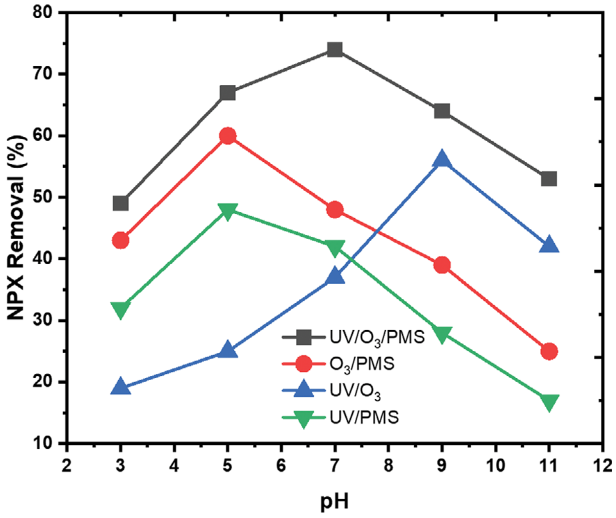

Fig. 3. Effect of pH on NPX degradation in UV/O$_3$/PMS process (O$_3$ dosage=5.1 mg/L, PMS dosage=0.84 mM/L, NPX concentration=5 mg/L).

decomposition of O_3 at various pH values. The effect of the solution pH on NPX degradation by different AOPs was investigated at different pH values (3, 5, 7, 9, and 11). As shown in Fig. 3, the removal percentage of NPX by UV/O_3/PMS, UV/PMS, O_3/PMS, and UV/O_3 processes reached 74%, 48%, 60%, and 56% within 30 min, respectively. In these situations, the optimum pH values were 7.0, 5.0, 5.0 and 9.0, for UV/O_3/PMS, UV/PMS, O_3/PMS, and UV/O_3 processes, respectively. The results revealed that the maximum degradation of NPX was obtained when the value of pH was equal to 7 in the UV/O_3/PMS process. In acidic conditions, the NPX removal percentage was at its lowest rate (49%). This can be explained by the fact that PMS-based AOPs can act effectively in a wide variety of pH, particularly at neutral pH. He et al. [22] investigated the β-lactam antibiotics degradation by UV/PMS process. They reported that reducing the pH values to 2-3 did not have any significant adverse effect on process performance and antibiotics degradation can be reached at a wide range of pH values. Furthermore, high concentrations of positive species at the acidic condition lead to an adverse effect on free radicals generation. Based on Eqs. (3)-(4), $^{\bullet}OH$ and $SO_4^{\bullet-}$ radicals are converted to ineffective and inactive states of HSO_4^- and H_2O in acidic conditions and this phenomenon could limit the degradation rate [23].

$$HO^{\bullet}+H^{+}+e^{-}\rightarrow H_2O \tag{3}$$

$$SO_4^{\bullet-}+H^{+}+e^{-}\rightarrow HSO_4^{-} \tag{4}$$

As observed in the equations, $^{\bullet}OH$ can be generated at higher pH values regarding the electron transfer reactions, due to the reaction of generated sulfate radicals with hydroxide alkalinity [24]. Accordingly, it can be concluded that the dominance of sulfate radical is decreased at alkaline conditions.

$$SO_4^{\bullet-}+OH^{-}\rightarrow SO_4^{2-}+^{\bullet}OH \tag{5}$$

In the UV/O_3/PMS process, $^{\bullet}OH$ are invariably co-present with $SO_4^{\bullet-}$. In addition, the ratio of $SO_4^{\bullet-}$ and $^{\bullet}OH$ radicals is dependent on pH of the solution. The increase or decrease of solution pH could overcome $SO_4^{\bullet-}$ and $^{\bullet}OH$ radicals balance. So, in the absence of hydroxide alkalinity, $SO_4^{\bullet-}$ is the main ROSs. On the other hand, in the presence of hydroxide alkalinity, $^{\bullet}OH$ is the dominant ROSs [25].

2-2. Effect of PMS Dosage

The effect of PMS dosage (0.1 to 2.66 mM L^{-1}) on NPX degradation in the UV/O_3/PMS process is shown in Fig. 4. Based on the figure, the photocatalytic degradation efficiency was 99.9% at the optimum dosage of PMS (1.68 mM L^{-1}). The removal efficiency of NPX increased linearly from 32% to 100% with increasing PMS dosage from 0.1 to 2.66 mM L^{-1}, which is in accordance with similar findings [26]. Increased generation of activated radicals, i.e., $^{\bullet}OH$ and $SO_4^{\bullet-}$ because of enhanced PMS activation by O_3 and UV led to a higher degradation of NPX. Nevertheless, Izadifard et al. [27] reported the removal of sulfolane between 1 to 3 g L^{-1} by the combination UV, O_3, and PDS. It is also reported that 2 g L^{-1} of PDS as an optimal value has been required. Moussavi et al. [28] reported that increasing the sulfate radical precursor leads to the enhancement of process performance until 200 mg L^{-1}. However, further increase of the initial concentration of PMS or PDS lowers the removal efficiency. The above points lead us to a self-quenching effect in a reactor containing $^{\bullet}OH$ and $SO_4^{\bullet-}$ due to higher concentration of the source of sulfate radicals, while this phenomenon is negligible under lower concentration of PMS or PDS.

2-3. Effect of O_3 Dosage for NPX Degradation

The influence of ozone dosage varying (2.1, 3.8, 5.1, 6.9, 8.2 and 9.5 mg L^{-1}) was studied as one of the important parameters in the UV/O_3/PMS process. As shown in Fig. 5, the maximum NPX degradation rate (95%) was obtained for UV/O_3/PMS process after 30 min of reaction. With the ozone process alone, only 19% of the NPX removal was achieved. Therefore, increasing the O_3 dosage enhanced NPX degradation and, as a result, it led to $^{\bullet}OH$ generation. However, the maximum degradation of NPX was obtained in 9.5 mg L^{-1} of the ozone concentration, but the optimum dosage of the ozone for achieving the best performance was selected

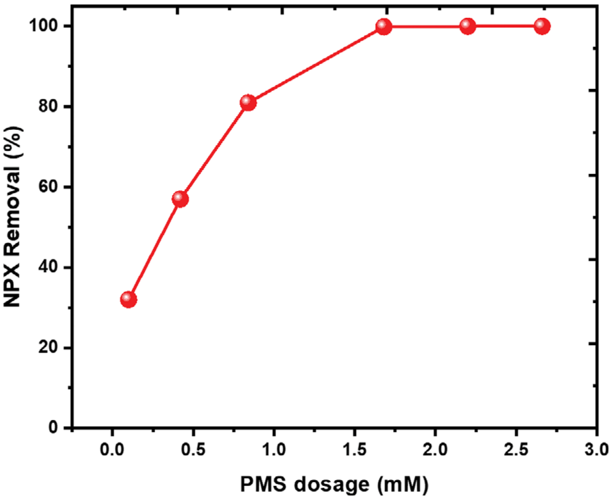

Fig. 4. Effect of PMS dosage on NPX removal in UV/O_3/PMS process (O_3=8.2 mg/L, NPX concentration=5 mg/L, reaction time =30 min and pH=7).

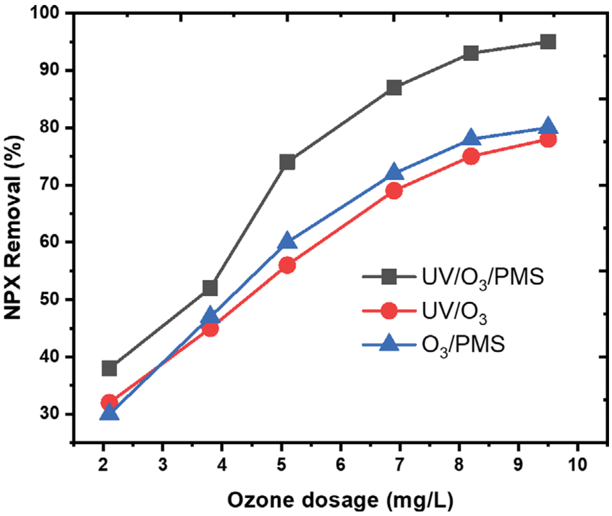

Fig. 5. The effect of O_3 dosage on NPX removal efficiency in UV/O_3/PMS process (PMS dosage=0.84 mM/L, NPX concentration=5 mg/L and time=30 min).

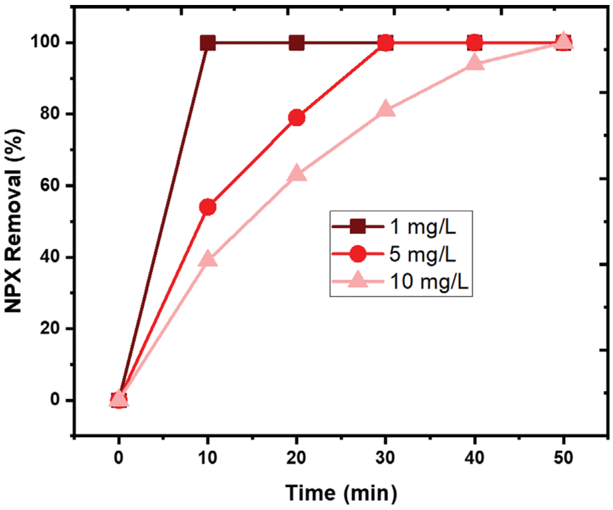

Fig. 6. Effect of initial NPX concentrations with reaction time in UV/O_3/PMS process (O_3 dosage=8.2 mg/L, PMS dosage=1.68 mM/L, pH=7).

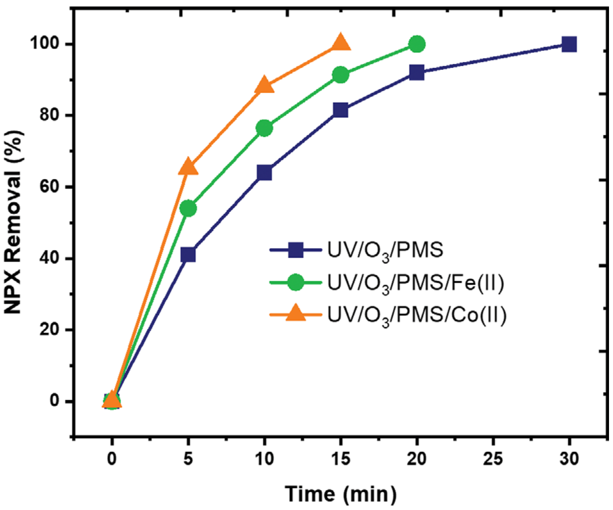

Fig. 7. Effect of transition metals on NPX degradation in UV/O_3/PMS process (O_3 dosage=8.2 mg/L, PMS dosage=1.68 mM/L, pH=7.0, Fe(II) and Co(II)=1 mM).

8.2 mg L^{-1}. Based on Eqs. (6) & (7), higher concentration of O_3 dosage as scavenger reacts with free radicals and reduces the removal efficiency of the contaminant [29].

$$O_3+HO^{\bullet}\rightarrow HO_2^{\bullet}+O_2 \tag{6}$$

$$O_3+SO_4^{\bullet-}\rightarrow SO_5^{\bullet-}+O_2 \tag{7}$$

Behnami et al. [30] investigated the ozone based advanced oxidation process. They also reported similar results in case of injected ozone concentrations. it is reported that the injected ozone concentration of 400 mg/h leads to the highest process performance in case of contaminant degradation and injected ozone concentration above this value does not positively affect the process, which is due the scavenging of the oxidizing agents by excess ozone concentration.

2-4. Effect of Initial NPX Concentration

Fig. 6 presents the degradation percentage of initial NPX concentration during reaction time. As can be seen, the removal efficiency declined with the rising of NPX concentrations. The removal efficiency for 1, 5, and 10 mg L^{-1} of NPX was obtained 100%, 79.9% and 61% after 20 min reaction time, respectively. However, complete degradation was achieved after 40 min for every value of NPX concentration ranging from 1 to 10 mg L^{-1}. It was assumed that the number of active radicals produced in the combination of UV, O_3, and PMS were constants as the O_3, PMS dosage, and pH were controlled at the optimum level in the UV reactor. Thus, the ratio of active radicals to NPX decreased at higher initial concentration in the present process [31]. The findings revealed that the combined UV/O_3/PMS process employed an efficient operation for eliminating wide concentrations of organic pollutants due to its superlative oxidation nature.

3. Combination of Transition Metal with UV/O_3/PMS Process on NPX Degradation

The effect of transition metals (Fe(II) and Co(II)) was investigated for the activation of common oxidants (O_3 and PMS) and generation of more reactive radicals with the objective of treating NPX in the UV/O_3/PMS process. Fe(II) and Co(II) generally serve as effective catalysts for activating O_3 and PMS due to the capability of operation at a wide range of pH, highest activity and low catalyst dosage for the activation process [32]. The performance of the UV/O_3/PMS process was evaluated for degradation of NPX in the absence and presence of Fe(II) and Co(II) ions (Fig. 7). The results illustrate that UV/O_3/PMS/Co(II) process was more efficient than UV/O_3/PMS/Fe(II) process. Thus, the elimination capability in the presence of transition metals is more effective than the pure PMS/O_3/UV process. Based on Eq. (8), Co(II) was also introduced as the best catalyst for the activation of PMS in the catalytical oxidation process.

$$Co(II)+HSO_5^{-}\rightarrow Co(III)+SO_4^{\bullet-}+HO^{-} \tag{8}$$

On the other hand, activation of O_3 by Co(II) ions to $^{\bullet}OH$ is well reported within Eq. (9) [26,33].

$$Co(II)+O_3+H_2O\rightarrow Co(OH)^{2+}+O_2+HO^{\bullet} \tag{9}$$

Therefore, it is confirmed that Co(II) ions can convert PMS into ROSs via the redox cycling of metal ions [34].

In conjunction with the activation of PMS with Fe(II) ions, the following equation applies [35].

$$Fe(II)+HSO_5^{-}\rightarrow Fe(III)+SO_4^{\bullet-}+HO^{-} \tag{10}$$

The presence of Fe(II) ions causes the acceleration of NPX degradation. This process has facilitated the conversion of Fe(III) to Fe(II) in the presence of UV irradiation via decomposition of generated iron complexes leading to the generation of hydroxyl radicals (Eqs. (11) & (12)) [36].

$$Fe(OH^{2+})+UV\rightarrow Fe^{2+}+HO^{\bullet} \tag{11}$$

$$Fe^{3+}+H_2O+UV\rightarrow Fe^{2+}+HO^{\bullet}+H^{+} \tag{12}$$

Based on Eqs. (11) & (12), PMS activation by O_3 and Fe(II) is considerably increasing the generation of reactive radical species. Furthermore, Fe(II) leads to the formation of Fe(IV), which is also a reactive species and is able to accelerate the process performance. Therefore, transition metals enhance the performance of the UV/O_3/PMS process concerning organic matters degradation (~100% of NPX removal). The effect of transitional metals such as F(II) has already been investigated in various AOPs. Moussavi et al. [37] reported the presence of Fe(II) in the Vacuum-UV process, which is both generation hydroxyl radical and ozone molecules. They reported that injection of 5 mg L^{-1} of Fe(II), increased the reaction rate constants in case of degradation of Cloxacillin for about 43%.

4. Effect of Scavenger and Water Matrix

The effect of scavengers and anions on the combination of O_3 and PMS in UV reactor for the NPX degradation was investigated to find how anions are affecting the process performance. In addition, the main pathway for PMS activation was identified by scavenging tests. These purposes were scrutinized by 1 mmol L^{-1} of anions (bicarbonate, chloride, nitrite, nitrate, and sulfate) and scavengers (EtOH, humic acid, TBA and NaN_3), which were separately added to the contaminant solution.

Fig. 8 illustrates the results of the effects of scavengers along with water matrix on NPX degradation. As shown in Fig. 8(a), ethanol, TBA and NaN_3 lead to a significant decrease in degradation efficiency. The degradation percentage of NPX declined from 100% to 25%, 28% and 30% in the presence of EtOH, TBA and NaN_3, respectively. EtOH is a strong scavenger for both sulfate radical (10^7 M^{-1} s^{-1}) and hydroxyl radical (10^9 M^{-1} s^{-1}), while TBA is a specific scavenger for hydroxyl radical ($3.8\text{-}7.6\times10^8$ M^{-1} s^{-1}) [38]. Accordingly, the difference in removal efficiency of NPX between TBA and EtOH represents the role of sulfate radicals. Therefore, in the present study, the role of sulfate radicals is slight. On the other hand, singlet oxygen may contribute in PMS-based AOPs. Self-decomposition of PMS is the main route of the generation of singlet oxygen. Moreover, the recombination of peroxymonosulfate radicals leads to the generation of sulfate radicals and singlet oxygen.

$$SO_5^{2-}+HSO_5^{-}\rightarrow HSO_4^{-}+SO_4^{2-}+1O_2 \tag{13}$$

$$SO_5^{\bullet-}+SO_5^{\bullet-}\rightarrow SO_4^{\bullet-}+SO_4^{\bullet-}+1O_2 \tag{14}$$

To determine the role of singlet oxygen, sodium azide is a powerful quencher with high reactivity to scavenge singlet oxygen. However, sodium azide also can quench sulfate radicals (2.5×10^9 M^{-1} s^{-1}) and hydroxyl radicals (1.2×10^{10} M^{-1} s^{-1}) significantly [39]. Hence, sodium azide is a versatile scavenger in SR-AOPs. As shown in Fig. 8(a), sodium azide suppressed the removal efficiency, indicating that all agents ($^1O_2$, $SO_4^{\bullet-}$ and $HO^\bullet$) are mainly responsible for the oxidation of NPX. But, regarding the results of TBA and EtOH, it is clear that the reduction in the efficiency corresponds to the hydroxyl radicals. Thus, it should be stated that the hydroxyl radicals are the major agents responsible for the degradation of NPX (Eq. (15)). Moreover, it is possible that the generated sulfate radical may be converted to hydroxyl radicals in the presence of water molecule (Eq. (16)).

$$HSO_5^{-}+O_3+H_2O+UV\rightarrow SO_4^{\bullet-}+3HO^{\bullet}+O_2 \tag{15}$$

$$SO_4^{\bullet-}+H_2O\rightarrow SO_4^{2-}+HO^{\bullet}+H^{+} \tag{16}$$

The presence of anions leads to a decrease of the NPX degradation rate on the UV/O_3/PMS process (Fig. 8). The addition of the

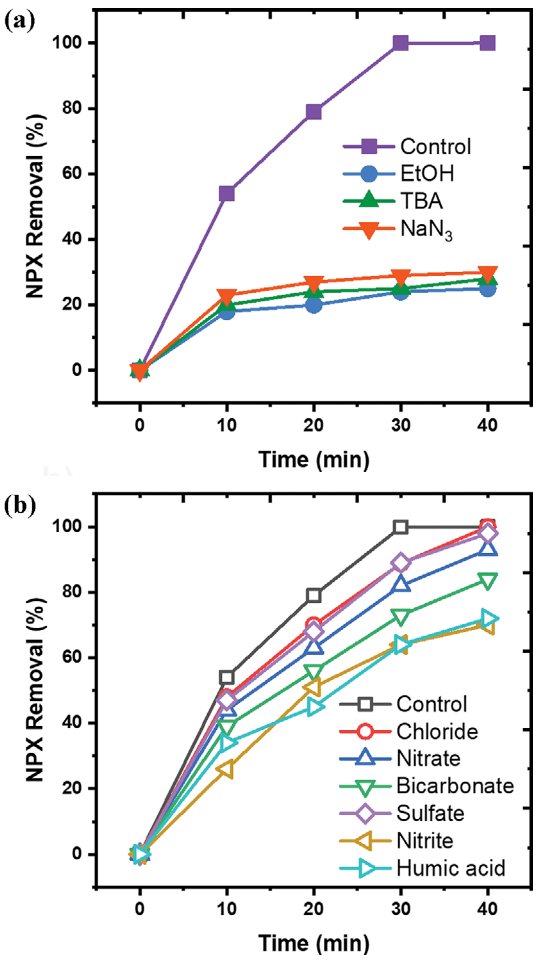

Fig. 8. Effect of different scavenger (a) and anions and humic acids (b) on NPX degradation in UV/O_3/PMS process.

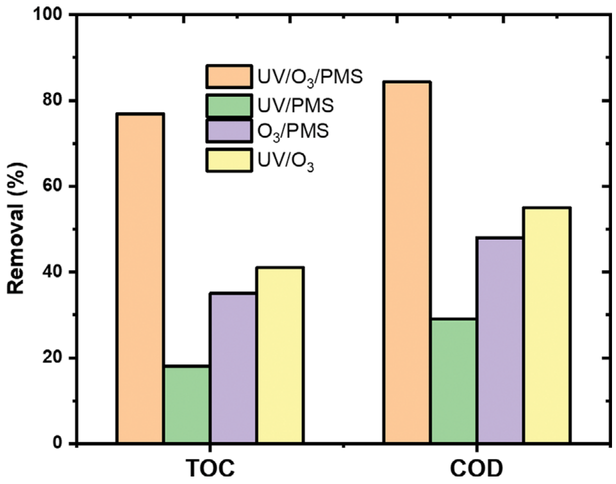

Fig. 9. COD and TOC removal with different processes (pH=5, PMS dosage=1.68 mM/L, O_3 dosage=8.2 mg/L and time=50 min).

anions resulted in the decrease of the NPX removal to 93%, 84%, 98% and 70% related to nitrate, bicarbonate, sulfate and nitrite, subsequently after 40 min of reaction, whereas in a solution without anions the degradation percentage reached 100% at the same reaction time. Humic acids also showed a high inhibitory effect on NPX degradation. Humic acids have high reactivity with free radicals, which can suppress the function of SR-AOPs. The competitive anions in the process preclude the degradation of naproxen,

Table 1. Identification of degradation intermediates of Naproxen by LC-MS (positive ion mode ESI mass spectra)

Intermediates	Degradation time (min)	m/z	Corresponding intermediates of dexamethasone
NPX	10	231	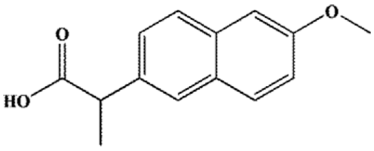
N1	10	275.3	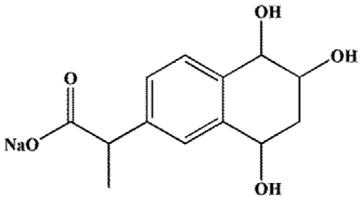
N2	10	259.1	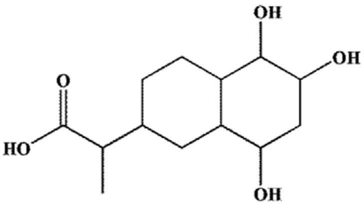
N3	10	307	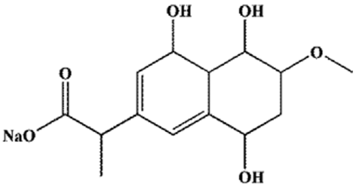
N4	20	205.1	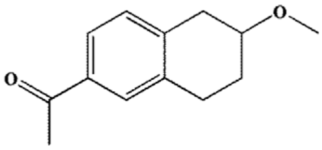
N5	20	191.3	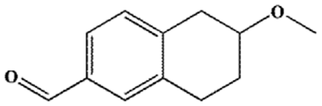
N6	20	179.3	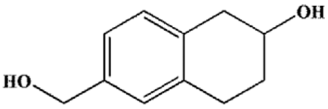
N7	20	165.2	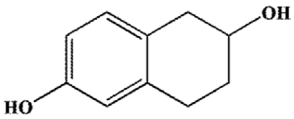
N8	40	143.1	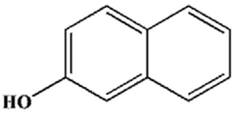
N9	60	125.3	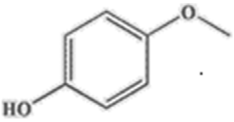

leading to a decrease in the removal efficiency. The anions could act as a radical scavenger, which react with hydroxyl radicals. The results were consistent with the other studies that anions reduced the degradation of pollutants [22,30]. He et al. [22] investigated the activation of persulfate by UV radiation for degradation of β-lactam antibiotics, and the effect various water anions was investigated on the presence of sulfate and hydroxyl radicals. They also reported that there is a slight reduction in the process performance in the presence of anions. It can be seen from Fig. 8 that the effects of the five anions on the degradation of NPX are different, and the order of inhibition of ions on the UV/O_3/PMS process is $NO_2^->$ humic acids$>HCO_3^->NO_3^->SO_3^{2-}>Cl^-$ due to the quenching effects of free radicals [40].

5. Comparison of Degradation and Mineralization

To scrutinize the degradation and mineralization of NPX in UV/O_3/PMS, UV/O_3, UV/PMS, and O_3/PMS processes, the same conditions were conducted to consider the effect of various processes on the COD and TOC removal efficiencies. As they are exhibited in Fig. 9, the removal of COD and TOC in the UV/PMS was lower than the other processes. Based on the literature, the ozone-

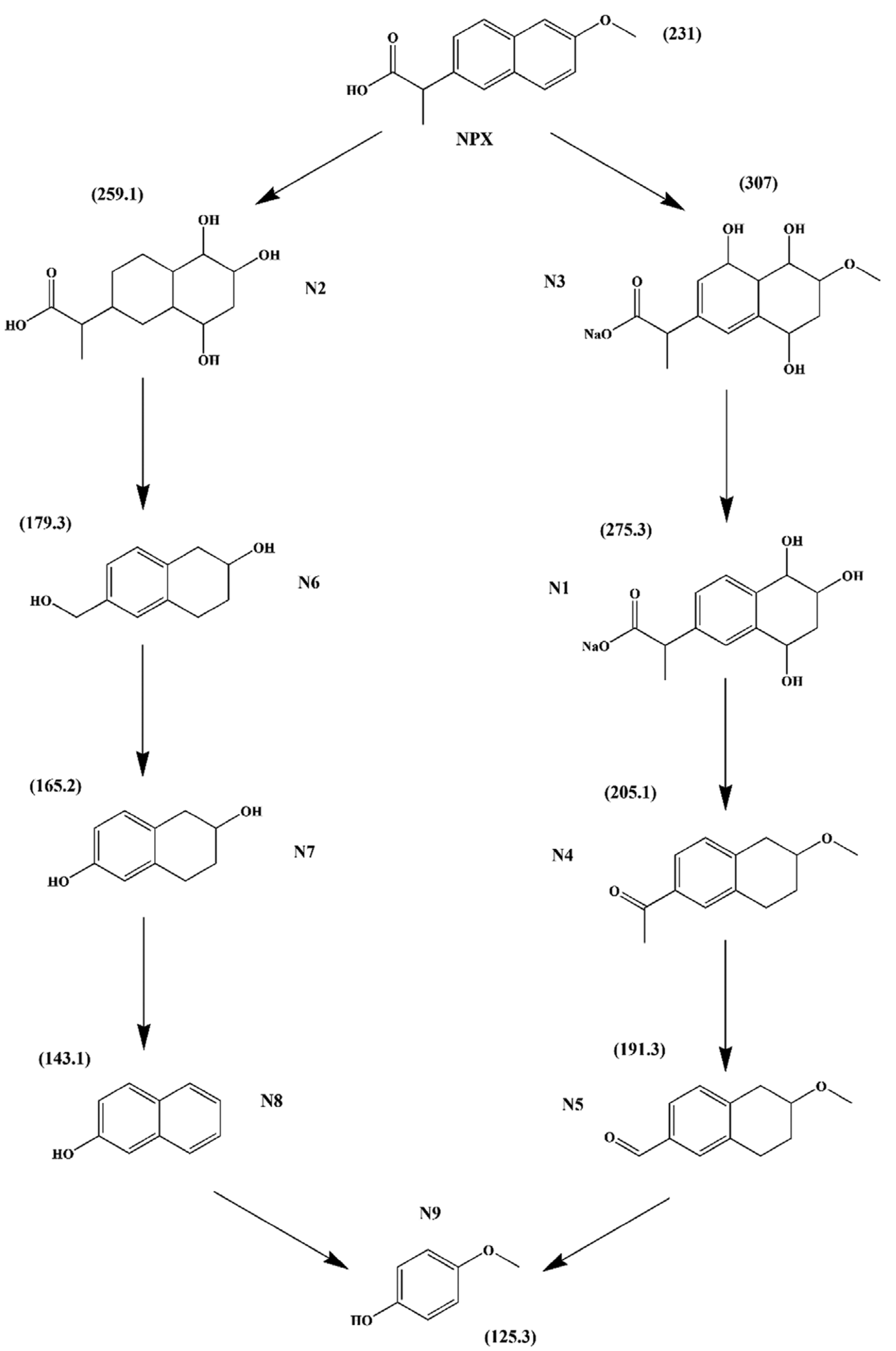

Fig. 10. Photodegradation pathway of NPX under visible light irradiation.

based processes are more effective than the combination of the oxidant and UV reactor including UV/PMS [41]. This is associated with the fact that the redox potential of ozone (2.01 V) is higher than that of PMS (1.82 V) and, thus, ozone can be more effective for degrading organic matter [42]. The decrease in COD and TOC by UV/PMS was 18% and 29%, respectively, while the O$_3$/PMS and UV/O$_3$ led to the removal of 35% and 41% concerning TOC and 48% and 55% of COD, respectively. This illustrates that ozone can significantly improve removal performance. With the combination of O$_3$ and the UV/PMS process, the removal efficiency of COD and TOC reached 84.3% and 76.9%, respectively. As a result, O$_3$ could efficiently activate PMS to COD and TOC removal, resulting in the generation of more free radicals.

The underlying mechanism of organic contaminants degradation in the UV/O$_3$/PMS system is based on various reactions [43]. PMS could be activated through UV radiation (Eq. (17)), thereby producing active radicals ($^\bullet$OH and $SO_4^{\bullet-}$).

$$HSO_5^- + UV \rightarrow SO_4^{\bullet-} + HO^\bullet \tag{17}$$

Also, UV radiation reveals an activation effect on ozone to create the hydroxyl radicals based on Eq. (18) [42]. Therefore, elimination of contaminants will occur via direct and indirect O$_3$ oxidation.

$$H_2O + UV + O_3 \rightarrow O_2 + 2HO^\bullet \tag{18}$$

Thus, O$_3$ plays two important roles. It acts as an oxidation agent and PMS activator. The reaction between the SO_5^{2-} of PMS and O$_3$ is responsible for $SO_5^{2-}O_3$ production (Eq. (19)) in which it is converted to $SO_5^{\bullet-}$ and $O_3^{\bullet-}$ radicals (Eq. (20)).

$$SO_5^{2-} + O_3 \rightarrow SO_5^{2-}O_3 \tag{19}$$

$$SO_5^{2-}O_3 \rightarrow 2SO_4^{\bullet-} + O_3^{\bullet-} \tag{20}$$

Sulfate radicals are efficiently produced using the reaction between $SO_5^{\bullet-}$ and O$_3$ (Eq. (21)), and the process progresses as follows (Eqs. (22) & (23)) [28]:

$$SO_5^{2-} + O_3 \rightarrow SO_4^{\bullet-} + 2O_2 \tag{21}$$

$$2SO_5^{\bullet-} \rightarrow 2SO_4^{\bullet-} + O_2 \tag{22}$$

$$2SO_5^{\bullet-} \rightarrow S_2O_8^{2-} + O_2 \tag{23}$$

Based on Eq. (24), UV radiation affects $O_3SO_5^{2-}$ to the generation of $^\bullet$OH and $SO_4^{\bullet-}$. With the decomposition of $O_3^{\bullet-}$ to $^\bullet$OH radicals (Eqs. (25) & (26)), the rate of degradation is increased. Among the reactive radicals produced during the above-mentioned reactions, $^\bullet$OH and $SO_4^{\bullet-}$ are the predominant species [44].

$$O_3SO_5^{2-} + 2H_2O + UV \rightarrow SO_4^{\bullet-} + O_2 + OH^- + 3HO^\bullet \tag{24}$$

$$O_3^{\bullet-} \leftrightarrow O^{\bullet-} + O_2 \tag{25}$$

$$O^{\bullet-} + H_2O \rightarrow HO^\bullet + HO^- \tag{26}$$

6. Degradation Intermediates of NPX and Proposed Pathway

To determine the intermediates of naproxen (m/z 231), the degradation products were identified by LC-MS. The positive ion mode (electro spray ionization mass spectra, ESI-MS) was performed and the m/z values and structure proposed for the nine main intermediates are summarized in Table 1. Based on the identified intermediates, the suggested degradation pathway of NPX is illustrated in Fig. 10. As shown, the N1 (m/z 275.3), N2 (m/z 259.1) and N3 (m/z 307) are hydroxylated products of NPX, which are formed by HO$^\bullet$ attacking, and increasing the reaction time to more than 10 min leads to the formation of the multi-hydroxylated intermediates [2]. After 20 min, these parent molecules disintegrate into the fragments with m/z values at 205.1, 191.3 and 179.3 (N4-N6), which are the products of the reduction of acetone groups and, as a result, the hydroxylation of aromatic rings [45]. Meanwhile, N6 may be formed by decarboxylation of N2, which is consistent with several studies [46]. As seen in the pathway, the HO$^\bullet$ may directly attack the methyl position of the naphthalene ring in NPX molecule and break the C–C$_{carboxyl}$ bond, which leads to the formation of N4 via the decarboxylation process [47]. The mineralization results of the final sample after 60 min degradation of NPX showed the cleavage of the naphthalene ring attacked by HO$^\bullet$ causes the formation of N9 with m/z value at 125.3. In summary, the LC-MS results confirmed hydroxylation and decarboxylation are the main pathways in NPX degradation.

7. Toxicity Assessment

Cytotoxicity measurement using MTT assay showed that NPX inhibited the viability of HEK 293T cells in comparison to control

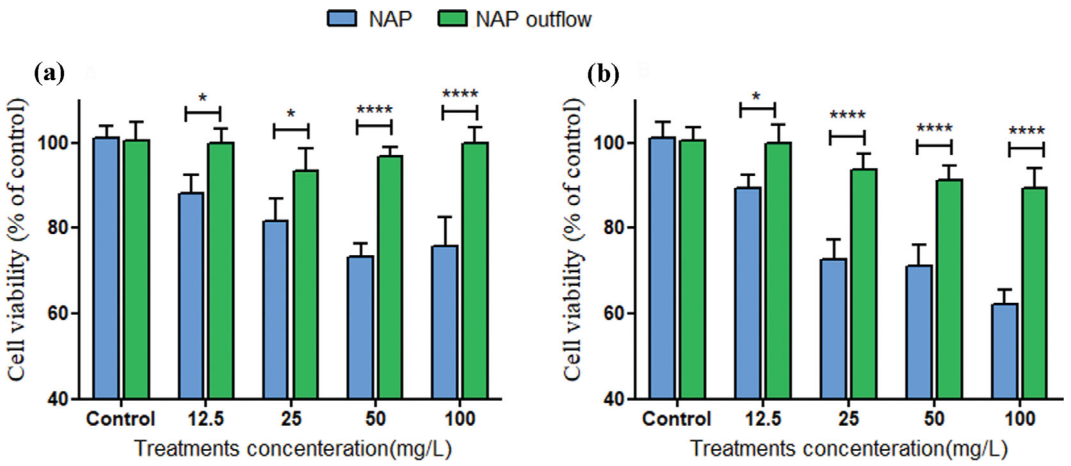

Fig. 11. Cytotoxicity assessment by MTT Assay in HEK 293T cells following the exposure of various concentrations of inlet NPX and NPX outflow for 24 h (a) and 48 (b). Values are mean±SD of three independent experiments. *p<0.05, **p<0.01, ***p<0.001, ****p<0.0001.

cell. As clearly seen in Fig. 11, the percent viability of cells treated with different concentrations of NPX significantly decreased compared to control group in 24 and 48 h (P≤0/05). Viability of the group treated with the 12.5, 25, 50 and 100 mg L^{-1} NPX decreased to 88.2±2.7%, 81.7±4.26%, 73.2±3.19% and, 75.31±6.7% compared to control (100%), respectively in 24 hours, while more viability reduction was shown after 48 hour. We also found that NPX outflow (all concentration and time) do not induce any toxicity to cells compared to control cells (p>0.05). The difference of cell viability between inlet and outflow in 12.5, 25, 50 and 100 μg L^{-1} was seen 11.6%, 11.7%, 23.6% and 24.3%, respectively, in 24 h and 10%, 18.12%, 20.16% and 27.1%, respectively, in 48 h. The results clearly suggest that treating the NPX in the investigated process significantly reduced its cytotoxicity, concluding that this process is an efficient method for complete detoxification of NPX drug.

8. Economic Evaluation

An economic evaluation was conducted to determine the operating cost required concerning the NPX degradation toward various processes. The operating cost for AOPs is primarily dependent on the cost of electricity for O_3 generation, power of the UV-lamp, oxygen generation as feed to O_3 generator, and chemicals. Because the costs of capital, labor, and maintenance are common for all advanced oxidation processes, they were excluded from the economic evaluation. In addition, for better understating the operation cost of NPX removal from wastewater, further experiments were conducted in a real wastewater matrix. For this purpose, hospital wastewater could better fit for this experiment. Accordingly, samples were taken from a local hospital wastewater treatment plant effluent. The samples were taken from the secondary settling tanks of an extended aeration process, and they were investigated in case of NPX concentrations. It was found that the NPX concentration in the samples was under detection limits. For conducting the experiments, a known amount of NPX was added to samples and the experiments were conducted based on the optimal conditions obtained in present study. The results of real wastewater samples are illustrated in Fig. 12. As shown, the oxidation time for the investigated processes almost doubled in the real wastewater. This is due to the presence of various organic and inorganic compounds in the samples. However, the results show that UV/O_3/PMS process is still able to completely oxidize the NPX in the solution.

Table 2. Operating costs for the AOPs reactor for 60 min and 300 mL NPX-laden wastewater

	Operating costs	US $
1	Cost of oxygen supply	0.00091
2	Cost of electricity for O_3 generation	0.000468
3	Cost of electricity for UV-lamp	0.00004
5	Cost of HSO_5^- addition	0.0324
	Operating cost for each process	US $/$m^3$
1	UV/O_3/HSO_5^-	112.72
2	HSO_5^-/UV	108.13
3	HSO_5^-/O_3	112.59
4	O_3/UV	4.72
5	HSO_5^-	108.00
6	O_3	4.59
7	UV	0.13

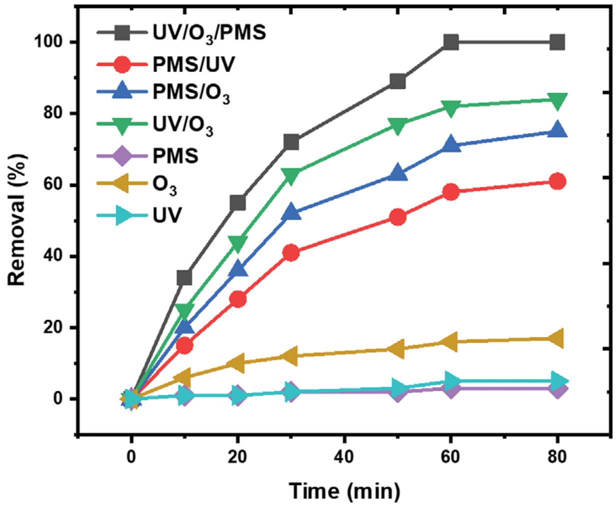

Fig. 12. The removal efficiencies of NPX in different processes in real wastewater matrix (O_3 dosage=8.2 mg/L, PMS dosage=1.68 mM/L, NPX concentration=5 mg/L, pH=5).

Table 2 presents the costs for electricity, oxygen generation, lamp replacement and PMS to operate the system in real wastewater samples. The operating costs in different processes followed the order: UV/O_3/PMS>PMS/O_3>PMS/UV>PMS alone>O_3/UV>O_3 alone> UV alone. Based on the maximum removal efficiency (99.9%) with the least amount of chemicals and energy consumption, the UV/O_3/PMS process is the best alternative for NPX removal. Since the reactivity between O_3 and PMS was low, and PMS was also expensive, PMS/O_3, O_3/UV, PMS alone and UV alone were energy-intensive processes for NPX degradation. Although the operation cost of the UV/O_3/PMS process was almost similar to that of others with PMS addition, this process can be appropriate to achieve a significant removal of organic pollutants. It is worth mentioning that other processes were not efficient for NPX removal.

CONCLUSION

The degradation of NPX via the UV/O_3/PMS, UV/O_3, UV/PMS, and O_3/PMS processes was comprehensively investigated. Under the conditions of PMS dosage=1.68 mM L^{-1}, O_3 dosage=8.2 mgL^{-1}, pH=7.0 and T=30 °C, the UV/O_3/PMS process indicated complete degradation of NPX in 30 min. The UV/O_3/PMS caused significant TOC and COD removal up to 76.9% and 84.3%, respectively. Primary active species that contributed to the NPX degradation were the $^{\bullet}OH$ and $SO_4^{\bullet-}$. The addition of transition metals (Fe(II) and Co(II)) enhanced the performance of the UV/O_3/PMS process, so that the removal efficiency reached 91.4% and 100% in the presence of Fe(II) and Co(II) ions, respectively. Additionally, various radical scavengers such as EtOH, TBA, humic acid and NaN_3 proved that $^{\bullet}OH$ and $SO_4^{\bullet-}$ species were the main oxidizing radicals for NPX removal. The mineralization results by the LC-MS illustrated that hydroxylation and decarboxylation were the main pathways in NPX degradation in the UV/O_3/PMS reactor. An economic evaluation of the operating costs of different oxidation processes for the real wastewater exhibited the UV/O_3/PMS is the most cost-effective process with considering the maximum removal percentage (112 US\$/m^3 for ≈100% of NPX removal). Finally, it is concluded that the UV/O_3/PMS process is a promising treatment option for the naproxen degradation.

ACKNOWLEDGEMENT

The authors gratefully acknowledge funding from the Abadan University of Medical Science with project No. 98U597.

REFERENCES

1. G.-M. A. Lucero, G.-M. Marcela, G.-M. Sandra, G.-O. L. Manuel and R.-E. Celene, *Water Air Soil Poll.*, **226**(6), 1 (2015).
2. S. Dong, X. Zhai, R. Pi, J. Wei, Y. Wang and X. Sun, *Water Sci. Technol.*, **81**(10), 2078 (2020).
3. L. Xu, X. Ma, J. Niu, J. Chen and C. Zhou, *J. Hazard. Mater.*, **379**, 120692 (2019).
4. Y. Yang, J. J. Pignatello, J. Ma and W. A. Mitch, *Water Res.*, **89**, 192 (2016); F. Rehman, M. Sayed, J. A. Khan, N. S. Shah, H. M. Khan and D. D. Dionysiou, *J. Hazard. Mater.*, **357**, 506 (2018).
5. H. Zangeneh, A. Zinatizadeh and M. Feizy, *J. Ind. Eng. Chem.*, **20**(4), 1453 (2014).
6. J. Wang and S. Wang, *Chem. Eng. J.*, **334**, 1502 (2018).
7. F. Jiang, B. Qiu and D. Sun, *Chem. Eng. J.*, **349**, 338 (2018).
8. X. Zhang, Z. Chen, J. Kang, S. Zhao, B. Wang, P. Yan, F. Deng, J. Shen and W. Chu, *J. Hazard. Mater.*, **401**, 123837 (2021).
9. Y. Shao, Z. Pang, L. Wang and X. Liu, *Molecules*, **24**(16), 2874 (2019).
10. Y. Mao, H. Dong, S. Liu, L. Zhang and Z. Qiang, *Water Res.*, **173**, 115615 (2020).
11. M. Khashij, M. Mehralian and Z. G. Chegini, *Pig. Resin Technol.*, **49**(5), 363 (2020).
12. Z. Yuan, M. Sui, B. Yuan, P. Li, J. Wang, J. Qin and G. J. E. S. W. R. Xu, *Environ. Sci-Wat. Res. Technol.*, **3**(5), 960 (2017).
13. Y. Cao, W. Qiu, Y. Zhao, J. Li, J. Jiang, Y. Yang, S.-Y. Pang and G. Liu, *Chem. Eng. J.*, **401**, 126 (2020).
14. Z. Lin, W. Qin, L. Sun, X. Yuan and D. Xia, *J. Water Process Eng.*, **38**, 101636 (2020).
15. Z. Liu, K. Demeestere and S. Van Hulle, *J. Environ. Chem. Eng.*, **9**(4), 105599 (2021).
16. APHA, *Federation, W. E., & APH Association. Standard methods for the examination of water and wastewater. American Public Health Association (APHA): Washington, DC, USA* (2005).
17. G. Moussavi, M. Pourakbar, S. Shekoohiyan and M. Satari, *Chem. Eng. J.*, **331**, 755 (2018).
18. Y. Ling, G. Liao, Y. Xie, J. Yin, J. Huang, W. Feng and L. Li, *J. Photoch. Photobio. A*, **329**, 280 (2016).
19. E. M. Cuerda-Correa, M. F. Alexandre-Franco and C. Fernández-González, *Water*, **12**(1), 102 (2020).
20. W. Qin, Z. Lin, H. Dong, X. Yuan, Z. Qiang, S. Liu and D. Xia, *Water Res.*, **186**, 116336 (2020).
21. S. Srithep and S. Phattarapattamawong, *Chemosphere*, **176**, 25 (2017).
22. X. He, S. P. Mezyk, I. Michael, D. Fatta-Kassinos and D. D. Dionysiou, *J. Hazard. Mater.*, **279**, 375 (2014).
23. Y.-H. Huang, Y.-F. Huang, C.-i. Huang and C.-Y. Chen, *J. Hazard. Mater.*, **170**(2), 1110 (2009).
24. E. Hayon, A. Treinin and J. Wilf, *J. Am. Chem. Soc.*, **94**(1), 47 (1972).
25. W.-D. Oh, Z. Dong and T.-T. Lim, *Appl. Catal. B-Environ.*, **194**, 169 (2016).
26. X. Liu, T. Zhang, Y. Zhou, L. Fang and Y. Shao, *Chemosphere*, **93**(11), 2717 (2013).
27. M. Izadifard, G. Achari and C. H. Langford, *Water Res.*, **125**, 325 (2017).
28. G. Moussavi, M. Pourakbar, E. Aghayani and M. Mahdavianpour, *Chem. Eng. J.*, **350**, 673 (2018).
29. L. Guo, Q. Zhong, J. Ding, M. Ou, Z. Lv and F. Song, *Ozone-Sci. Eng.*, **38**(5), 382 (2016).
30. A. Behnami, J.-P. Croué, E. Aghayani and M. Pourakbar, *RSC Adv.*, **11**(58), 36965 (2021).
31. Y. Xu, Y. Wu, W. Zhang, X. Fan, Y. Wang and H. Zhang, *Chem. Eng. J.*, **353**, 626 (2018).
32. J. Deng, Y. Ge, C. Tan, H. Wang, Q. Li, S. Zhou and K. Zhang, *Chem. Eng. J.*, **330**, 1390 (2017).
33. I. H. Chowdhury, A. H. Chowdhury, P. Bose, S. Mandal and M. K. Naskar, *RSC Adv.*, **6**(8), 6038 (2016).
34. J. Lim and M. R. Hoffmann, *Environ. Sci-Nano*, **7**(5), 1602 (2020).
35. D. L. Ball and J. O. Edwards, *J. Phys. Chem.*, **62**(3), 343 (1958).
36. L. Clarizia, D. Russo, I. Di Somma, R. Marotta and R. Andreozzi, *Appl. Catal. B-Environ.*, **209**, 358 (2017).
37. G. Moussavi, M. Rezaei and M. Pourakbar, *Chem. Eng. J.*, **332**, 140 (2018).
38. G. Moussavi, M. Pourakbar, E. Aghayani, M. Mahdavianpour and S. Shekoohyian, *Chem. Eng. J.*, **294**, 273 (2016).
39. Y. Zhou, J. Jiang, Y. Gao, J. Ma, S.-Y. Pang, J. Li, X.-T. Lu and L.-P. Yuan, *Environ. Sci. Technol.*, **49**(21), 12941 (2015).
40. Y. Kanigaridou, A. Petala, Z. Frontistis, M. Antonopoulou, M. Solakidou, I. Konstantinou, Y. Deligiannakis, D. Mantzavinos and D. I. Kondarides, *Chem. Eng. J.*, **318**, 39 (2017); X. Gao, Q. Guo, G. Tang, W. Peng, Y. Luo and D. He, *J. Water Reuse Desal.*, **9**(3), 301 (2019).
41. C. V. Rekhate and J. K. Srivastava, *Chem. Eng. J. Adv.*, **3**, 100031 (2020).
42. M.-S. Chou and K.-L. Chang, *Ozone-Sci. Eng.*, **29**(5), 391 (2007).
43. J. Sharma, I. M. Mishra, D. D. Dionysiou and V. Kumar, *Chem. Eng. J.*, **276**, 193 (2015); M. Scott, G. J. Millar and A. Altaee, *J. Water Process Eng.*, **31**, 100806 (2019).
44. G. Liu, X. Li, B. Han, L. Chen, L. Zhu and L. C. Campos, *J. Hazard. Mater.*, **322**, 461 (2017).
45. F. Méndez-Arriaga, J. Giménez and S. Esplugás, *J. Adv. Oxid. Technol.*, **11**(3), 435 (2008).
46. D. Kanakaraju, C. A. Motti, B. D. Glass and M. Oelgemöller, *Chemosphere*, **139**, 579 (2015).
47. C.-J. M. Chin, T.-Y. Chen, M. Lee, C.-F. Chang, Y.-T. Liu and Y.-T. Kuo, *J. Hazard. Mater.*, **277**, 110 (2014).